



Cite this: DOI: 10.1039/d0gc01449d

Pseudopeptidic macrocycles as cooperative minimalistic synzyme systems for the remarkable activation and conversion of CO₂ in the presence of the chloride anion†

 Ferran Esteve,^a Belén Altava,^a M. Isabel Burguete,^a Michael Bolte,^b Eduardo García-Verdugo^{*,a} and Santiago V. Luis^{*,a}

A series of pseudopeptidic compounds have been assayed as organocatalysts for the conversion of CO₂ into organic carbonates through a cooperative multifunctional mechanism. Conformationally constrained pseudopeptidic macrocycles **3a** and **3b** have been revealed to be excellent synzymes for this purpose, being able to provide a suitable preorganization of the different functional elements and reaction components to activate the CO₂ molecule and stabilize the different anionic intermediates involved, through a series of cooperative supramolecular interactions. As a result, remarkable catalytic efficiencies are found at low CO₂ pressures and moderate temperatures, with TON and TOF values surpassing those reported for other organocatalytic supramolecular systems under similar conditions. The process works well for monosubstituted epoxides. The involvement of the different structural elements has been analyzed in detail and preliminary studies show the potential for recovery and reuse of these catalytic systems.

Received 27th April 2020,
Accepted 27th June 2020

DOI: 10.1039/d0gc01449d

rsc.li/greenchem

1. Introduction

Nature has developed smart and complex systems working under elaborate self-regulation protocols and mild conditions and producing reduced waste. Many of them are based on the self-organization and self-assembly of a few simple building blocks.¹ Clear examples are provided by enzymes, which are highly sophisticated catalysts that Nature has optimized over billions of years. Their unique self-organization affords specific 3D-arrangements of individual functional groups allowing the required supramolecular and cooperative interplay of the various active-site functionalities within the enzyme. This often enables a precise location of the reacting substrates/reagents within the 3D-environment of the active site of the enzyme leading to highly efficient transformations in terms of both activity and selectivity.²

Developing abiotic systems able to mimic the efficiency of these natural structures is an important goal in Green Chemistry,³ and a broad range of synthetic supramolecular systems displaying enzymatic activity, often referred to as synzymes, has been reported.⁴ As in natural enzymes, the catalytic activity of these systems can provide selective substrate recognition and is dominated by supramolecular interactions.⁵ In this field, macrocyclic cavities have been often exploited as minimalistic enzymatic mimics, taking advantage of the higher degree of preorganization of the functionalities present, which represents a key element of the active sites of enzymes.⁶

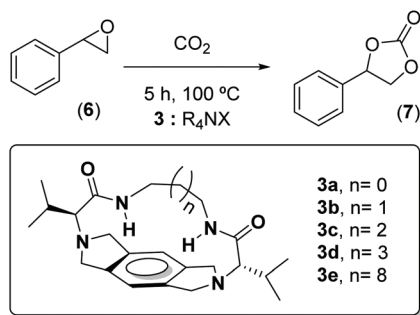
Achieving such a preorganization is not always easy and macrocyclizations often represent a synthetic challenge.⁷ However, efficient macrocyclization strategies based on conformational, configurational or template-induced self-organization have been developed for the preparation of minimalistic macrocyclic pseudopeptides.^{8,9} Despite their simplicity, as well as the high molecular diversity attainable and the presence of a high level of well-defined functionality,¹⁰ these macrocycles have not been yet exploited as supramolecular organocatalytic systems.

On the other hand, the conversion of CO₂ into valuable chemicals represents a challenge of great current interest in Green Chemistry, from different perspectives.¹¹ A variety of catalytic approaches have been reported for the reaction between CO₂ and epoxides to form cyclic carbonates,^{12–15} a family of compounds of interest for a variety of different applications.¹⁶ Here we report the initial results for the evaluation

^aDepartamento de Química Inorgánica y Orgánica, Universitat Jaume I, Av. Sos Baynat s/n, 12071 Castellón, Spain. E-mail: cepeda@uji.es, luiss@uji.es

^bInstitut für Anorganische Chemie, J. W. Goethe-Universität Frankfurt, 60438 Frankfurt/Main, Germany

† Electronic supplementary information (ESI) available: Synthesis of pseudopeptides; comparison of catalytic systems; solvent and cation effect; studies for the interaction with anions; kinetic profiles; conformational study of the macrocyclic compounds; study of the catalytic mixtures; substrate scope for the CO₂ addition; ¹H, ¹³C NMR, and HRMS spectra for **5**; XRD and computational data (PDF). CCDC 1995455. For ESI and crystallographic data in CIF or other electronic format see DOI: 10.1039/d0gc01449d



Scheme 1 Cycloaddition of carbon dioxide to styrene oxide catalysed by the supramolecular systems **3**: R_4NX .

of some macrocyclic pseudopeptidic systems (**3**, Scheme 1), in the presence of tetra-alkyl-ammonium chlorides, as supramolecular synzymes for the activation and conversion of CO_2 into carbonates in the presence of epoxides. When appropriately adjusted, the different structural elements of these minimalistic pseudopeptides like the nature of the central spacers, the amino acid side chains, and the groups attached to the amino functions, can facilitate a precise and well-defined self-assembly of the halide, the epoxide and CO_2 in a minimalistic cooperative supramolecular interplay with the macrocyclic host, providing a highly efficient catalytic transformation of CO_2 into the corresponding cyclic carbonates.

2. Experimental

General

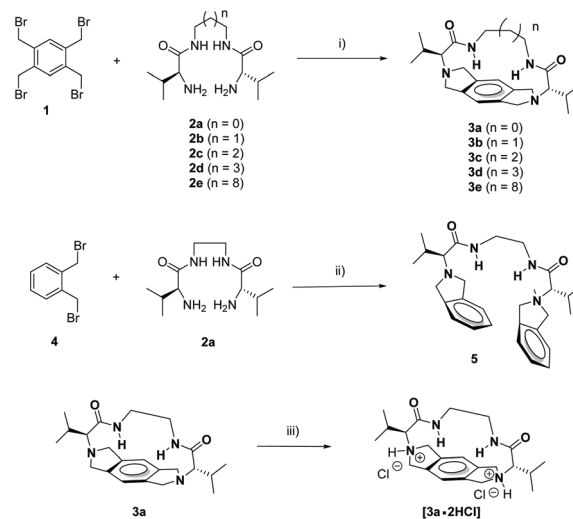
NMR experiments were carried out at 500, 400 or 300 MHz for 1H and 125, 100 or 75 MHz for ^{13}C . Chemical shifts are reported in ppm from tetramethyl silane, using the residual solvent resonance as the internal standard. Fourier transform infrared spectra (FT-IR) were recorded using an attenuated total reflection (ATR) adapter. High resolution mass spectrometry (HRMS) was recorded with a Q-TOF instrument. Rotatory power was determined with a digital polarimeter (Na: 589 nm). Melting points were measured using a standard apparatus and are uncorrected.

Open chain pseudopeptidic compounds **2** were prepared following literature procedures,^{8c} as well as the macrocyclic structures **3** (Scheme 2).¹⁷

Two different set-ups were used for the cycloaddition reaction with CO_2 . The first one, employed for the reaction at atmospheric pressure, used a standard round bottom flask with a CO_2 balloon (100% CO_2) as gas supply. The second one, for the reactions under pressure, used a Berghof R-300 high pressure reactor connected to a pressurized CO_2 source and a back-pressure regulator from Jasco (see Fig. S11†)

Synthesis of (2*S*,2'*S*)-*N,N'*-(ethane-1,2-diyl)bis(2-(isoindolin-2-yl)-3-methylbutanamide

Synthesis of 5. Compound **2a** (101 mg, 0.391 mmol) and α,α' -dibromo-*o*-xylene (**4**) (215 mg, 0.782 mmol) were dissolved



Scheme 2 Synthesis of macrocyclic systems and related analogues. (i) CH_3CN , 2–3 h, 90 °C. (ii) CH_3CN , 5 h, 90 °C. (iii) CH_3OH , 1 h, 25 °C.

in acetonitrile (65 mL) in the presence of Cs_2CO_3 (764 mg, 2.346 mmol), and the reaction mixture was refluxed on a heating mantle with magnetic stirring for 5 hours. The solvent was then evaporated under vacuum and the resulting residue was treated with basic water (pH \approx 11), to afford pure **5** as a solid after centrifugation of the resulting suspension at 3000 rpm for 8 min. Yield (140 mg, 77.3%, 0.302 mmol); m.p. = 168–169 °C; $[\alpha]_D^{25} = -41.7^\circ$ ($c = 0.4$, CH_3CN); IR (ATR): 3297, 2959, 1641, 1544 cm^{-1} ; 1H NMR (400 MHz, CD_3CN) $\delta = 0.91$ (d, $J = 6.7$ Hz, 6H), 0.98 (d, $J = 6.8$ Hz, 6H), 2.86 (d, $J = 6.7$ Hz, 2H), 3.29–3.33 (m, 4H), 3.95–4.03 (m, 8H), 7.00 (s, 2H), 7.15–7.22 (m, 8H), $^{13}C\{^1H\}$ -NMR (100 MHz, CD_3CN) $\delta = 18.4$, 20.4, 29.8, 39.9, 56.5, 74.1, 123.1, 127.5, 140.8, 172.4; HRMS (ESI/Q-TOF) m/z : $[M + H]^+$ calcd for $C_{28}H_{38}N_4O_2$ 463.3703; found 463.3706.

General procedure for the reaction of 6 with CO_2 in the presence of pseudopeptides and Bu_4NCl

8.7 mmol of styrene oxide, 0.087 mmol of Bu_4NCl and 0.0087 mmol of the corresponding pseudopeptide were added to a 25 mL twin-necked round bottom flask. The system was purged with dry N_2 and CO_2 , leaving two CO_2 balloons (100% CO_2) as gas supply. The mixture was refluxed on a heating mantle with magnetic stirring for 5 hours at 100 °C. Finally, a sample of the crude was collected and analyzed by NMR. The conversion of **6** into **7** could be calculated, considering the integration of the signal at 5.67 ppm for the disappearance of **6** and the one for the signal at 3.88 ppm for the formation of **7**.

IR kinetic experiments

The same procedure above was carried out, but using just one CO_2 balloon (100% CO_2) and closing the second neck with a septum. Samples at defined times were directly collected through the septum with a syringe and directly analysed by FT-IR. The conversion of **6** into **7** could be calculated, using

the area of the bands at 1440–1510 cm^{-1} ($\nu_{\text{C-C}}$ stretching, aromatic ring) as the reference and the area of the band at 1020–1100 cm^{-1} ($\nu_{\text{C-O}}$ asymmetric vibration) for the formation of 7.

Crystal structures

Single crystals suitable for X-ray crystallography were obtained by slow evaporation of a methanol solution of [3a·2HCl]. A crystal was selected and mounted on a SuperNova, Dual, Cu at zero, Atlas diffractometer. The structure was solved with the SHELXT 2014/5¹⁸ structure solution program and refined with the SHELXL-2018/3¹⁹ refinement package. Artwork representations were processed using MERCURY²⁰ software. The refined structure of [3a·2HCl] has been registered in CCDC with the deposition number 1995455.†

Molecular modelling

Lowest energy conformations for the different species considered were calculated at the MMFF level of theory using Spartan08.²¹ Stationary points were confirmed by subsequent frequency calculation. All vibrational frequencies were positive.

3. Results and discussion

In previous supramolecular catalytic systems evaluated for this process, a common strategy has been the use of supramolecular hosts able to strongly bind cations, affording in this way activated anions (e.g. “naked” X^-),^{22–24} In the present case, however, the design elements for the organocatalytic pseudopeptides considered took into account their multifunctional and highly preorganized character and their capacity to develop cooperative supramolecular interactions with the three species involved in the process: the nucleophilic species (halide anions), the epoxide and the CO_2 molecules. Such interactions could include $\text{NH}_{\text{amide}} \cdots \text{X}^- \cdots \text{HN}_{\text{amide}}$, $\text{O}_{\text{epoxide}} \cdots \text{HN}_{\text{amide}}$ and $\text{N}_{\text{amine}} \cdots \text{CO}_2$ and cooperate to locate the three components in close proximity (A1, Fig. 1), within a supramolecular complex, and with an appropriate orientation as to facilitate low energy pathways for the desired reaction, fully mimicking the behaviour of many enzymatic sites.

A common mechanism reported for the activation of CO_2 has been its interaction with a Lewis base, in particular tertiary amines.^{25,26} Thus, the $\text{N}_{\text{amine}} \cdots \text{CO}_2$ interaction can also contribute to this activation (A2, Fig. 1). Besides, Brønsted or Lewis acid sites have been used to activate the epoxide,²⁷ sometimes involving bifunctional or multifunctional systems,^{15b,28,29} and accordingly the $\text{O}_{\text{epoxide}} \cdots \text{HN}_{\text{amide}}$ can contribute to activate the epoxide. The selected synzymatic structure 3 has a high modularity (size of the macrocyclic cavity, conformational preferences, polarity, etc.) as to enable a fast optimization of the catalytic efficiency.

Constrained macrocycles 3, prepared as previously reported from open chain C_2 -symmetric pseudopeptides 2 and tetrakis(bromomethyl)arenes 1 (Scheme S1†), have two amide groups appropriately located as to cooperatively interact with anions

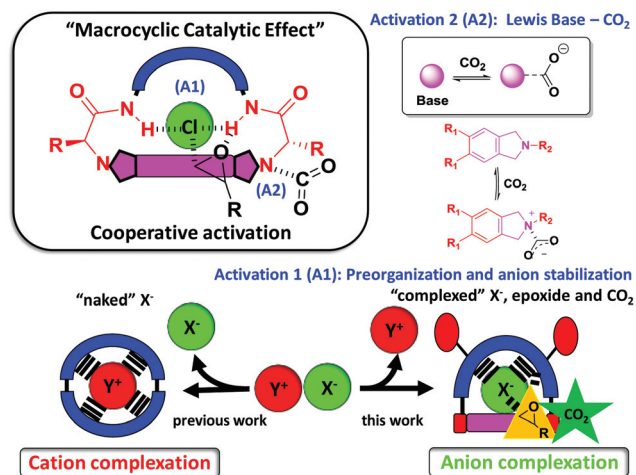


Fig. 1 Pseudopeptidic macrocycles as minimalistic synzymes for the conversion of CO_2 through a cooperative multifunctional activation mechanism. A1: preorganization of the reactive components (amide and amine sites). A2: activation of the inert CO_2 species by a Lewis base (amine sites).

and potentially with the oxygen atom of epoxides, and in close proximity of conformationally restricted amino groups that could participate in the activation of CO_2 molecules.¹⁷

Following this design, the pseudopeptidic macrocycle 3a was initially tested in combination with Bu_4NX salts for the synthesis of the organic carbonate 7 (Scheme 1). The selection of the L-valine derivative was based in the excellent results observed in the synthesis of 3a from 2a and in the suitability of its solubility properties, as most of these pseudopeptidic compounds have a rather limited solubility in styrene oxide (SO). The results obtained from the initial screening at 100 °C and ambient pressure (CO_2 balloon) using 3a and SO as an epoxide of moderate-low reactivity,^{13a} are summarized in Table 1. After 5 h and in the absence of the macrocycle, conversions into carbonate were 49% for Bu_4NI , 59% for Bu_4NBr and 65% for Bu_4NCl (entries 1–3, Table 1). It must be noted that in the absence of the tetrabutylammonium salt no reaction took place when 3a was added (entry 4, Table 1). The use, under the same conditions, of an equimolar mixture of both 3a and Bu_4NX (1 mol% each relative to 6) led to a significant increase in the activity in the case of Bu_4NCl , reaching a 93% conversion (entry 7, Table 1) while the observed improvements were minor for Bu_4NBr and Bu_4NBr (entries 5 and 6, Table 1). A complete selectivity towards the formation of 7 was observed and the formation of other species was not detected by NMR. The decomposition of tetraalkylammonium salts has been reported in some catalytic processes involving the same reaction, but the formation of tributyl amine was not detected up to the detection limit of the techniques used.³⁰ It should be also noted that the crude of reactions with conversion close or lower than 50% were also analysed by chiral HPLC. In all the cases, neither the epoxide nor the carbonate showed any enantioselectivity excluding the enantiopreference of the

Table 1 Screening of **3a**/ Bu_4NX mixtures for the reaction between styrene oxide (**6**) and CO_2 to afford **7**^a

Entry	Bu_4NX (mol%)	3a (mol%)	Conversion ^b (%)	TON (Bu_4NX)	TON (3a)
1	X = I, (1)	—	49	49	—
2	X = Br, (1)	—	59	59	—
3	X = Cl, (1)	—	65	65	—
4	—	1	4	—	4
5	X = I, (1)	1	53	53	53
6	X = Br, (1)	1	67	67	67
7	X = Cl, (1)	1	93	93	93
8	X = Cl, (1)	0.1	93	93	930
9	X = Cl, (0.1)	0.1	22	220	220
10	X = Cl, (0.1)	—	16	160	—
11	X = Cl, (0.1) ^c	—	45	450	—
12	X = Cl, (0.1) ^c	0.1	73	730	730
13	X = Cl, (0.1) ^c	0.01	76	760	7600

^a 1 mL epoxide **6** (8.7 mmol), $p(\text{CO}_2) = \text{CO}_2$ balloon, 100 °C, 5 h.

^b Conversions determined by ¹H NMR, selectivity for **7** was >99.9% in all cases. ^c $p(\text{CO}_2) = 10$ bar.

macrocycle for a given enantiomeric epoxide, which seems reasonable considering the temperatures used.

The same high conversion was maintained when the amount of macrocycle was reduced from 1 to 0.1 mol%, while keeping a 1 mol% loading of Bu_4NCl (entry 8, Table 1). However, in this case, the TON with respect to the **3a** was significantly higher, reaching a value of 930. Reducing also the loading of Bu_4NCl to 0.1 mol%, keeping a 1:1 **3a**: Bu_4NCl molar ratio, led to an important reduction in conversion (22%, entry 9, Table 1). When the same experiment was performed at 10 bar of CO_2 , a 73% conversion was observed. This result highlighted again the synergic effects between Bu_4NCl and the macrocycle **3a**, as in the absence of the macrocycle only a 45% conversion was observed (entries 11 and 12, Table 1).

A *ca.* 1.5 times increase in conversion was always observed, for all the conditions assayed, when 1 equivalent of **3a** was added to Bu_4NCl . At 10 bar of CO_2 the amount of macrocycle could be further reduced to 0.01 mol%, while keeping a 1:10 **3a**: Bu_4NCl molar ratio, with the conversion to carbonate being 76% after 5 h. This represents achieving excellent TON and TOF values of 7600 and 1520 h^{-1} . Although some comparable or higher TON and TOF values have been described for transition metal-based catalysts (Table S2†), often at higher pressures and temperatures,^{14,31} the results presented here significantly surpass those found for organocatalytic and supramolecular catalytic systems, in particular when epoxides of moderate-low reactivity like SO are involved (for a detailed comparison see Table S1†).^{22,23,27–29} Some remarkable examples of organocatalytic systems being able to achieve high conversions/yields of cyclic carbonates (>90%) at ambient pressure and temperature have been reported. It must be noted, however, that most often they involve the use of more reactive epoxides like glycidyl or propylene oxides and, besides, commonly use 2–10% catalyst loadings and extended reaction times (20–24 h) which leads to significantly reduced TON and TOF values.^{25,27–29}

The catalytic performance of several tetraalkylammonium chlorides (R_4NCl) in the presence or absence of **3a** was also assayed (Table S3†). For both Bu_4NCl and Et_4NCl the presence of the macrocycle **3a** (0.1 mol%) led again to an increase in conversion of *ca.* 1.5 times and to good TON values of 930 and 800, respectively (entries 4 and 5, Table S3†). However, no reaction was observed for Me_4NCl , most likely for the lack of solubility of this salt in the reaction medium (entry 6, Table S3†).

Although the initial solvent free conditions should be preferred according to the principles of green chemistry, the reaction was also studied in 2-MeTHF and acetonitrile (Table S4†). Both are non protic polar solvents in which nucleophiles can be relatively “free” making them more reactive. The lack of an adequate solubility of the ammonium salt and the macrocycle precluded an efficient reaction in 2-MeTHF. Results improved, however, in acetonitrile. At 1 bar of CO_2 and 80 °C, with a 2.4 M concentration of epoxide, the conversion was 18% after 3 h in the presence of 1 mol% of Bu_4NCl and was increased more than three times when 0.1 mol% of **3a** was added (60% conversion, entries 5 and 6, Table S4†). When using only 0.01 mol% of macrocycle **3a**, the conversion after 3 h reached 39%, which again corresponds with excellent TON and TOF values of 3900 and 1300 h^{-1} , respectively (entry 7, Table S4†).

As mentioned above, entries 1–3 in Table 1 reveal that for the **3a**: Bu_4NX system the reactivity order was $\text{Cl}^- > \text{Br}^- \gg \text{I}^-$. This follows the basicity order and not the nucleophilicity order as found for other supramolecular receptors.^{23c} Being the more basic anion, chloride is expected to interact stronger with receptors **3** through hydrogen bonding to the amide NH fragments, as shown in related pseudopeptides,^{8,32} and this should make chloride less available to react. Thus, the mechanism involved cannot rely on the activation of the nucleophile, but on the capacity of **3a** to correctly preorganize all the reacting species at short distances and with the correct orientation as to significantly enhance the reaction rate. The stronger binding of Cl^- (in comparison with Br^- and I^-) can favour the adoption of the required conformation in the macrocyclic pseudopeptide not achievable with the other two anions.

Thus, ¹H NMR titrations in benzene-*d*₆ (ESI, Fig. S1†) showed that upon addition of Bu_4NCl , the NH amide proton signal underwent a large downfield shift ($\Delta\delta = 2.74$ ppm). This variation is consistent with the development of strong $\text{NH}_{\text{amide}} \cdots \text{Cl}^- \cdots \text{HN}_{\text{amide}}$ H-bonding interactions ($\log \beta = 3.15 \pm 0.01$). The interaction of **3a** with other halide anions was much smaller. After addition of 10 equivalents of Bu_4NX the observed downfield shifts for the amide protons ($\Delta\delta_{\text{NH}}$) were 1.43 and 0.19 ppm for Br^- and I^- , respectively (Table S5†). The corresponding binding constants were too low to be accurately determined. Significant changes were also observed for the signals corresponding to the methine of the stereogenic carbon ($\Delta\delta = 0.87$ ppm), to the aromatic protons ($\Delta\delta = 0.39$ ppm) and to one of the isoindolinic protons -appearing as two AB systems in the 3.3–4.6 ppm region-that shifted downfield from 3.42 ppm to 4.32 ppm, strongly reducing the anisochrony of the AB system (ESI, Fig. S1 and S2†). Overall, this

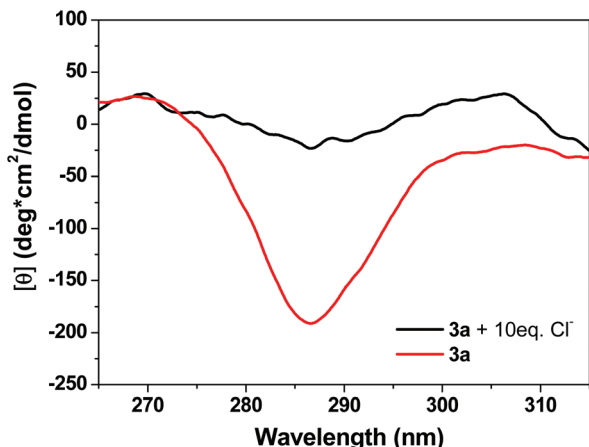


Fig. 2 CD spectra in benzene (0.5 mM) for **3a** (red) and **3a** + 10 equivalents of Bu_4NCl (black).

suggests important conformational changes upon complexation with Cl^- .

In the same way, the strong negative signal at 285 nm observed in the CD of **3a** in benzene (0.5 mM) essentially disappeared after addition of 10 equivalents of Bu_4NCl (Fig. 2) while the effect was less intense in the presence of Bu_4NBr and minor for Bu_4NI (ESI, Fig. S3†). This CD signal is assignable to π - π^* transitions of the aromatic group located in a chiral environment and, as well known from studies related to proteins and other biomolecules, is very sensible to changes in the environment and mobility and to the presence of additional groups at short distances.³³

Molecular modelling of the $[\mathbf{3a} + \text{Cl}^-]$ complex shows that in the most stable conformation both amide groups of the macrocycle adopt a *syn* disposition and strongly interact with the halide anion (Fig. 3).²¹ The conformation observed in the macrocycle is similar to the one found in its X-Ray structure,¹⁷ although the two carbonyl groups display longer distances to the corresponding methylene groups of the isoindolinic rings, in particular in one of the cases (ESI, Fig. S4†) which agrees well with the changes observed in ^1H NMR.

In contrast, for the most stable conformation calculated for the $[\mathbf{3a} + \text{I}^-]$ complex, the amide groups adopt an *anti*-disposition, where only one amide group is interacting with the iodide anion (Fig. 3). It must be noted that only in the *syn*-disposition of the amide groups it is possible to facilitate the

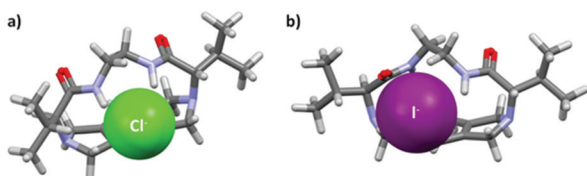


Fig. 3 Lowest energy conformers calculated for (a) $[\mathbf{3a} + \text{Cl}^-]$ complex highlighting the amide groups are in *syn*-disposition. (b) $[\mathbf{3a} + \text{I}^-]$ complex highlighting the amide groups in *anti*-disposition.

location of the epoxide on the same side of the halide and close to the activated CO_2 as envisaged in the catalyst design.

The level of structural preorganization of **3a**, being a conformationally constrained macrocycle can be relevant for the results obtained. To evaluate a possible “*macrocyclic effect*”,³⁴ the open chain pseudopeptidic compound **5**, displaying the same functional groups and the same connectivity than **3a**, but lacking the constraints associated to the macrocyclic structure, was synthesized (Scheme S1†) and tested.

The course of the model reaction catalysed by Bu_4NCl or by this salt in the presence of **3a** or **5** (0.1 equivalents relative to Bu_4NCl) was monitored by FT-ATR-IR spectroscopy (ESI, Fig. S5†). The conversion vs. time profiles confirmed the importance of the macrocyclic structure, showing that the higher conversion obtained after 5 h for the supramolecular system **3a**: Bu_4NCl (65% for Bu_4NCl alone, 73% in the presence of **5** and 93% in the presence of **3a**) was associated to a faster reaction rate (Fig. 4). Thus, for instance, after one hour of reaction TOF values reached 380 h^{-1} for Bu_4NCl , 480 h^{-1} for **5**: Bu_4NCl and 630 h^{-1} for **3a**: Bu_4NCl .

The results shown in Fig. 4 also confirmed the importance of the tertiary amine groups in the activation of CO_2 molecules.^{25,26} When the related pseudopeptide **2a** presenting primary amino groups was assayed, an irrelevant catalytic effect was observed (Fig. 4). Furthermore, the double salt $[\mathbf{3a}\cdot 2\text{HCl}]$, was obtained by treatment of **3a** with the stoichiometric amount of HCl in methanol (Scheme S1†). This salt could maintain the main structural features of $[\mathbf{3a} + \text{Cl}^-]$ but lacking the activating role of the tertiary amines. The ^1H NMR spectrum of this salt in $\text{DMSO-}d_6$ (ESI, Fig. S6†) showed the appearance of a new signal for the ammonium proton ($\text{R}_3\text{N}^+\text{H}$) at 10.45 ppm. Additionally, the amide signal was shifted downfield ($\Delta\delta_{\text{NH}} = 1.3 \text{ ppm}$), indicating the presence of $\text{NH}_{\text{amide}}\cdots\text{Cl}^-$ interactions. The X-Ray crystal structure of $[\mathbf{3a}\cdot 2\text{HCl}]$ contained two molecules in the asymmetric unit, with *syn* and *anti*-arrangements of the amide groups (ESI,

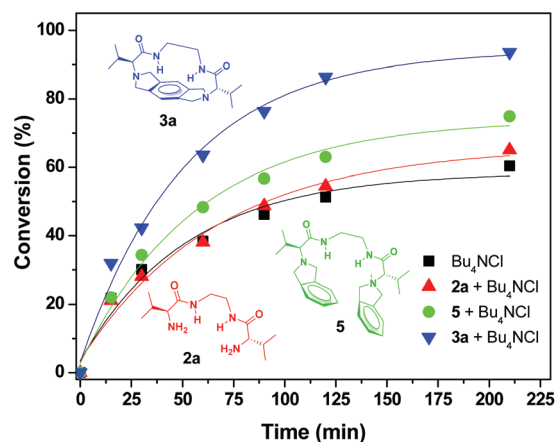


Fig. 4 Conversion vs time profiles obtained for the reaction between **6** and CO_2 as monitored by FT-ATR-IR. Catalysts: 1 mol% Bu_4NCl and 0.1 mol% of **2a**, **3a** or **5**. Reaction conditions: solventless, 100°C , 5 h, CO_2 balloon.

Fig. S7, see also Fig. S12†). Both structures exhibit $\text{Cl}^- \cdots \text{HN}_{\text{amide}}$ hydrogen bonds, particularly the one with the *syn* amide groups that seems to display an appropriate preorganization of the cavity. However, no formation of the carbonate **7** was obtained when **6** was heated in the presence of 1 mol% of salt [**3a**·2HCl], highlighting the importance of these tertiary amino groups.

The length of the central aliphatic spacer linking the two amino acid fragments is another structural element defining the conformational flexibility of compounds **3** and, accordingly, their level of preorganization. Hence, important differences were found as a function of the length of the spacer in macrocycles **3a–e** demonstrating that a reduction in the preorganization of the macrocyclic cavity is critical, leading to less active systems. Compounds with shorter spacers ($n = 0$ or 1, **3a** and **3b**) afforded efficient catalytic systems (conversion > 90%, entries 1 and 2, Table 2), while for spacers of intermediate length ($n = 2$ or 3, **3c** and **3d**) some decrease in conversion was observed (*ca.* 80% conversion, entries 3 and 4, Table 2). Finally, the macrocycle with the largest spacer ($n = 8$) afforded a strong decay in activity (52% conversion, entry 5, Table 2).

The increase in mobility associated to the length of the spacer in compounds **3** was highlighted by the changes observed for the signals from the four protons of the isoindolinic rings in ^1H NMR spectra. As mentioned, they are observed in all solvents as two well-differentiated AB systems, the signals for the protons directed towards the macrocyclic cavity, and accordingly affected by the shielding cone of the $\text{C}=\text{O}_{\text{amide}}$ fragments, appearing at higher field. In CD_3OD (ESI, Fig. S2†), the larger anisochrony was observed for compounds with the shorter spacers (**3b**, $\Delta\delta = 0.59$ and 0.37) and decreased significantly for the macrocycles with the larger spacers (**3d** and **3e**). For **3e** the spectrum changes to an apparent AB single system, suggesting a high degree of conformational flexibility allowing the rotation of the aromatic unit, accompanied by the inversion at the nitrogen atoms, with respect to the macrocyclic main plane.³⁵

Besides, the CD spectrum for the less active macrocycle **3e** (larger spacer) was like that of **3a** but, in this case, the effect of the addition of Bu_4NCl was minor. For the intermediate macrocycle **3d** the CD signal was essentially absent, which can

be associated to the coexistence of several conformations as suggested by X-Ray data and molecular modelling studies,¹⁷ and no significant changes were observed in the presence of chloride anion (ESI, Fig. S3†). Thus, the formation of a strong [**3a** + Cl^-] complex displaying a highly restricted conformational mobility and an appropriate preorganization seems to be a requisite for the higher activity of **3a** in this catalytic process, despite the reduced reactivity of the anion in such a complex. The larger spacers would allow, for instance, and *anti*-disposition of the amide groups and the location of chloride and epoxide coordinated on opposite sides of the macrocyclic cavity, precluding a direct interaction of these two components of the reaction.

According to literature data, hydrogen bonding between the oxygen atom of SO and the amide hydrogens can activate the epoxide.^{15,28,29} ^1H NMR titrations of **3a** with **6** in C_6D_6 did not show significant changes that could be attributed to the formation of the corresponding complex. However, ^1H NMR spectra obtained for the [**3a** + Cl^- + **6**] system in benzene- d_6 in ratios similar to those in the catalytic experiments (2 mM of **3a**, 20 mM of Bu_4NCl and 240 mM of **6**) suggested the formation of a ternary complex (ESI, Fig. S8†). Thus, the complex signal for the methylene protons closer to the ammonium ($\text{R-CH}_2\text{-N}^+\text{R}_3$) experienced an upfield shift ($\Delta\delta = 0.05$ ppm), associated to the weakening of the ion pair, that is appreciably larger than the one observed in the absence of **6**. Despite the large excess of **6** present, a minor downfield shift was also observed for the protons of the epoxide ring suggesting the presence of a weak interaction $\text{Cl}^- \cdots \text{HCHOR}_{\text{epoxide}}$.

In agreement with this, molecular modelling for [**3a** + Cl^- + **6**] showed that in the lowest energy species the rigidly preorganized cavity of **3a** facilitates a cooperative but asymmetric H-bonding of both *syn*-amide groups with the chloride anion, while **6** is located displaying short $\text{NH}_{\text{amide}} \cdots \text{O}$ distances, adopting a suitable conformation for the nucleophilic attack on the less hindered carbon atom and contributing to the shielding of the anion from its interaction with Bu_4N^+ (Fig. 5a).

In contrast, in the lowest energy species for [**3e** + Cl^- + **6**] only one of the two *anti*-amides interacts with the chloride anion, while the epoxide is located closer to the macrocycle but adopting an orientation much less favourable for the reaction to occur, as the CO_2 molecule that could be interacting with one of the amino groups should not be appropriately located (Fig. 5b).

In the light of the former results, the observed catalytic activity seems to rely on a cooperative multifunctional mechanism based on an efficient preorganization of the different components and participating groups: amide, tertiary amine, anion, epoxide and CO_2 (ESI, Fig. S9†). According to the general mechanism established for the synthesis of cyclic carbonates from epoxides and carbon dioxide, the mechanism depicted in Fig. 6 can be considered.³⁰ After formation of the [**3a** + Cl^-] complex (**A**), interaction with the epoxide can lead to the formation of the [**3a** + Cl^- + **6**] supramolecular species (**B**), while CO_2 can be activated by tertiary amino groups in close

Table 2 Screening of macrocyclic catalysts for the reaction between styrene oxide (**6**) and CO_2 to afford **7**^a

Entry	Macrocyclic ^b	Spacer -(CH ₂) _{n+2} -	3 : Bu_4NCl molar ratio	Conversion ^c (%)
1	3a	0	1 : 10	93
2	3b	1	1 : 10	96
3	3c	2	1 : 10	83
4	3d	3	1 : 10	79
5	3e	8	1 : 10	52

^a 1 mL of **6** (8.7 mmol), 1 mol% of Bu_4NCl , 1 : 10 macrocycle : Bu_4NCl molar ratio, CO_2 balloon, 100 °C, 5 h. Conversion achieved for Bu_4NCl alone 65%. ^b Obtained as previously reported in ref. 17. ^c Conversions determined by ^1H NMR; selectivity for **7** was >99.9 % in all the cases.

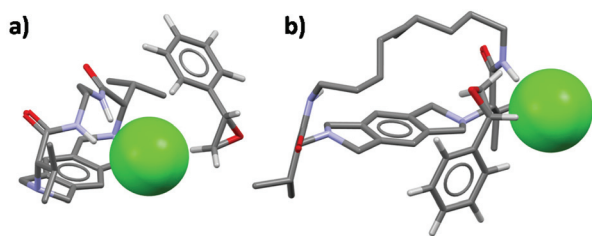


Fig. 5 Lowest energy conformers calculated (MMFF level of theory) for the supramolecular species (a) $[3a + Cl^- + 6]$ and (b) $[3e + Cl^- + 6]$. Non-essential hydrogen atoms are omitted for clarity.

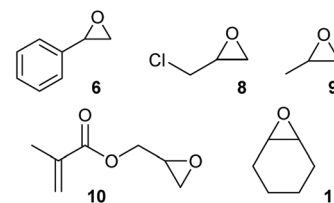


Fig. 7 Structures of the epoxides assayed.

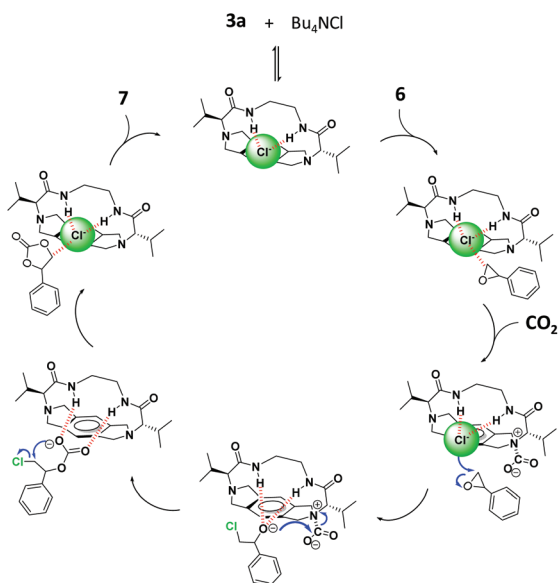


Fig. 6 Proposed mechanism for the cycloaddition of styrene oxide and CO_2 catalysed by the supramolecular system $3a : R_4NX$.

proximity leading to the intermediate C. The attack of the chloride to the less hindered carbon atom of the epoxide produces the requisite intermediate D, which subjected to the insertion of CO_2 generates the intermediate E. Both, the alkoxide and the alkylcarbonate anions, in intermediates D and E, can be stabilised by interaction with the amide groups, reducing the energy required for the ring-opening of the epoxide, which is considered the rate determining step. Finally, the corresponding cyclic carbonate is obtained through an intramolecular cyclization step to give the $[3a + Cl^- + 7]$ species (F), from which the catalytic $[3a + Cl^-]$ complex (A) is regenerated. Nevertheless, more detailed studies, including in depth kinetic analyses and high level computational studies, are needed to fully analyze these mechanistic details, although this is out of the scope of this initial work.

The coupling reactions of CO_2 with several epoxides (Fig. 7) were also investigated under the optimized conditions. In general, excellent conversions (>90%) were found for reactive and moderately reactive monosubstituted epoxides (entries 1–4, Table 3). Only for cyclohexene oxide a lower conversion

Table 3 Cycloaddition of CO_2 to different epoxides catalysed by $3a : Bu_4NCl^a$

Entry	Epoxide	Conversion ^b (%)	TON (3a)	TON (Bu_4NCl)
1	6	93	930	93
2	8	94	940	94
3	9	99	990	99
4	10	98	980	98
5	11	18 (99) ^c	180 (990) ^c	18 (99) ^c

^a Reaction conditions: solventless, 100 °C, 5 h, CO_2 balloon; 1 mol% of Bu_4NCl , 0.1 mol% of $3a$. ^b Conversions determined by 1H NMR. ^c Conversions determined by 1H NMR after 15 h of reaction without solvent, 100 °C using a CO_2 balloon.

was observed (18%), as a result of its lower reactivity associated to the steric hindrance present (entry 5, Table 3).³⁶ In this case, 15 hours were required for a complete conversion of the epoxide in the desired carbonate.

Finally, the reusability of the catalyst was also assayed using styrene oxide as the substrate at the optimized reaction conditions (Fig. S10[†]). The pseudopeptidic macrocycle $3a$ could be recovered almost quantitatively by precipitation with cyclopentyl methyl ether (CPME) and could be used after centrifugation and decantation of the solution with only a minor decrease in the conversion of 6 into 7 being observed after three reuses. After the recycling protocol, the integrity of the organocatalyst was corroborated by NMR and MS analyses, with no significant changes observed as compared to the spectra of freshly prepared $3a$. Considering the small scale of the experiments, these results support the feasibility of this methodology to isolate and reuse the catalytic system.

4. Conclusions

Overall, the present results show that pseudopeptidic macrocycles represent a remarkable and unique scaffold for the development of a synzymatic approach allowing the efficient conversion of CO_2 into organic carbonates achieving high TON and TOF values surpassing the best values reported for supramolecular systems under related conditions. Despite the reduced reactivity that could be associated to the interaction of the chloride anion with the amide NH fragments, the conformational restrictions defined by the macrocyclic structure, along with the very high functional density, facilitate an appropriate supramolecular preorganization, with suitable distances

and orientations, of the three components involved: the nucleophilic anion, the epoxide and one molecule of CO₂. Simultaneously, the tertiary amino groups can activate the CO₂ molecules, while the amide functionalities could activate the epoxide and stabilize the different anionic intermediates formed, leading to the cooperative involvement of the different structural elements, fully mimicking the behaviour found in enzymatic sites. Similar catalytic activities are observed for monosubstituted epoxides, while the activity decreases with cyclohexene oxide. A preliminary approach has been developed allowing the recovery and reuse of the catalytic system. Additional work is needed to fully disclose the mechanistic aspects of the process involved, but the present results provide a new promising entry to the development of efficient metal-free processes for the conversion of CO₂ into cyclic carbonates from epoxides.

Conflicts of interest

There are no conflicts to declare.

Acknowledgements

This work has been partially supported by projects UJI-B2019-40 (Pla de Promoció de la Investigació de la Universitat Jaume I) and RTI2018-098233-B-C22 (Ministerio de Ciencia, Innovación y Universidades). F.E. acknowledges MECD for the FPU fellowship. The authors are grateful to the SCIC of the Universitat Jaume I for technical support.

Notes and references

- (a) Z. Huang, S. K. Kang, M. Banno, T. Yamaguchi, D. Lee, C. Seok, E. Yashima and M. Lee, *Science*, 2012, **337**, 1521–1526; (b) V. Schaller and A. R. Bausch, *Nature*, 2012, **481**, 268–269; (c) K. H. Smith, E. Tejeda-Montes, M. Poch and A. Mata, *Chem. Soc. Rev.*, 2011, **40**, 4563–4577; (d) J. S. Moore and M. L. Kraft, *Science*, 2008, **320**, 620–621; (e) R. A. Segalman, *Science*, 2008, **321**, 919–920.
- A. Fersht, *Structure and Mechanism in Protein Science: A Guide to Enzyme Catalysis and Protein Folding*, W. H. Freeman, New York, 1999.
- (a) L. Wang, R. Zhang, Q. Han, C. Xu, W. Chen, H. Yang, G. Gao, W. Qin and W. Liu, *Green Chem.*, 2018, **20**, 5311–5317; (b) X. Cao, S. P. Teong, D. Wu, G. Yi, H. Su and Y. Zhang, *Green Chem.*, 2015, **17**, 2348–2352; (c) G. Rothenberg and J. H. Clark, *Green Chem.*, 2000, **2**, 248–251.
- (a) E. Kuah, S. Toh, J. Yee, Q. Ma and Z. Gao, *Chem. – Eur. J.*, 2016, **22**, 8404–8430; (b) Z. Dong, Q. Luo and J. Liu, *Chem. Soc. Rev.*, 2012, **41**, 7890–7908; (c) M. J. Wiester, P. A. Ulmann and C. A. Mirkin, *Angew. Chem., Int. Ed.*, 2011, **50**, 114–137.
- (a) Y. Zhu, J. Rebek and Y. Yu, *Chem. Commun.*, 2019, **55**, 3573–3577; (b) N. W. Wu, I. D. Petsalakis, G. Theodorakopoulos, Y. Yu and J. Rebek, *Angew. Chem., Int. Ed.*, 2018, **57**, 15091–15095; (c) N. W. Wu and J. Rebek, *J. Am. Chem. Soc.*, 2016, **138**, 7512–7515.
- (a) B. D. Nath, K. Takaishi and T. Ema, *Catal. Sci. Technol.*, 2020, **10**, 12–34; (b) M. Raynal, P. Ballester, A. Vidal-Ferran and P. W. N. M. van Leeuwen, *Chem. Soc. Rev.*, 2014, **43**, 1734–1787.
- V. Martí-Centelles, M. D. Pandey, M. I. Burguete and S. V. Luis, *Chem. Rev.*, 2015, **115**, 8736–8834.
- (a) V. Martí-Centelles, M. I. Burguete and S. V. Luis, *J. Org. Chem.*, 2016, **81**, 2143–2147; (b) V. Martí-Centelles, M. I. Burguete and S. V. Luis, *Chem. – Eur. J.*, 2012, **18**, 2409–2422; (c) J. Becerril, M. Bolte, M. I. Burguete, F. Galindo, E. Garcia-España, S. V. Luis and J. F. Miravet, *J. Am. Chem. Soc.*, 2003, **125**, 6677–6686.
- (a) M. Bru, I. Alfonso, M. Bolte, M. I. Burguete and S. V. Luis, *Chem. Commun.*, 2011, **47**, 283–285; (b) I. Alfonso, M. Bolte, M. Bru, M. I. Burguete, S. V. Luis and J. Rubio, *J. Am. Chem. Soc.*, 2008, **130**, 6137–6144.
- S. V. Luis and I. Alfonso, *Acc. Chem. Res.*, 2014, **47**, 112–124.
- (a) L. Delafontaine, T. Asset and P. Atanassov, *ChemSusChem*, 2020, **13**, 1688–1698; (b) M. Ronda-Lioret, G. Rothenberg and N. R. Shiju, *ChemSusChem*, 2019, **12**, 3896–3914; (c) P. Tomkins and T. E. Mueller, *Green Chem.*, 2019, **21**, 3994–4013; (d) Y. Chen and T. Mu, *Green Chem.*, 2019, **21**, 2544–2574; (e) J. Leclair and D. J. Heldebrant, *Green Chem.*, 2018, **20**, 5058–5081; (f) Q.-W. Song, Z.-H. Zhou and L.-N. He, *Green Chem.*, 2017, **19**, 3707–3728; (g) G. Fiorani, W. Guo and A. W. Kleij, *Green Chem.*, 2015, **17**, 1375–1389.
- (a) R. R. Shaikh, S. Pornpraprom and V. D'Elia, *ACS Catal.*, 2018, **8**, 419–450; (b) M. Alves, B. Grignard, R. Mereau, C. Jerome, T. Tassaing and C. Detrembleur, *Catal.: Sci. Technol.*, 2017, **7**, 2651–2684; (c) H. Buttner, L. Longwitz, J. Steinbauer, C. Wulf and T. Werner, *Top. Curr. Chem.*, 2017, **375**, 50.
- (a) S. Subramanian, J. Oppenheim, D. Kim, T. S. Nguyen, W. M. H. Silo, B. Kim, W. A. Goddard III and C. T. Yavuz, *Chem*, 2019, **5**, 3232–3242; (b) Y. Xie, Z. Zhang, T. Jiang, J. He, B. Han, T. Wu and K. Ding, *Angew. Chem., Int. Ed.*, 2007, **46**, 7255–7258.
- (a) K. Takaishi, B. D. Nath, Y. Yamada, H. Kosugi and T. Ema, *Angew. Chem., Int. Ed.*, 2019, **58**, 9984–9988; (b) J. A. Castro-Osma, K. J. Lamb and M. North, *ACS Catal.*, 2016, **6**, 5012–5025; (c) C. Maeda, T. Taniguchi, K. Ogawa and T. Ema, *Angew. Chem., Int. Ed.*, 2015, **54**, 134–138; (d) M. M. Dharman, J.-I. Yu, J.-Y. Ahn and D.-W. Park, *Green Chem.*, 2009, **11**, 1754–1757.
- (a) H. Zhou, H. Zhang, S. Mu, W.-Z. Zhang, W.-M. Ren and X.-B. Lu, *Green Chem.*, 2019, **21**, 6335–6341; (b) Y.-D. Li, D.-X. Cui, J.-C. Zhu, P. Huang, Z. Tian, Y.-Y. Jia and P.-A. Wang, *Green Chem.*, 2019, **21**, 5231–5237.
- (a) A. J. Kamphuis, F. Picchioni and P. P. Pescarmona, *Green Chem.*, 2019, **21**, 406–448, DOI: 10.1039/c8gc03086c;

- (b) X. Liu, J. G. de Vries and T. Werner, *Green Chem.*, 2019, **21**, 5248–5255; (c) N. Yadav, F. Seidi, D. Crespy and V. D'Elia, *ChemSusChem*, 2019, **12**, 724–754; (d) Y. Ding, J. Tian, W. Chen, Y. Guan, H. Xu, X. Li, H. Wu and P. Wu, *Green Chem.*, 2019, **21**, 5414–5426.
- 17 F. Esteve, B. Altava, M. Bolte, M. I. Burguete, E. García-Verdugo and S. V. Luis, *J. Org. Chem.*, 2020, **85**, 1138–1145.
- 18 G. M. Sheldrick, *Acta Crystallogr., Sect. A: Found. Crystallogr.*, 2008, **64**, 112–122.
- 19 G. M. Sheldrick, *Acta Crystallogr., Sect. C: Struct. Chem.*, 2015, **71**, 3–8.
- 20 C. F. Macrae, I. J. Bruno, J. A. Chisholm, P. R. Edgington, P. McCabe, E. Pidcock, L. Rodriguez-Monge, R. Taylor, J. van de Streek and P. A. Wood, *J. Appl. Crystallogr.*, 2008, **41**, 466–470.
- 21 (a) B. J. Deppmeier, A. J. Driessen, T. S. Hehre, W. J. Hehre, J. A. Johnson, P. E. Klunzinger, J. M. Leonard, I. N. Pham, W. J. Pietro and Y. Jianguo, *Calculated using Spartan08 software at the MMFF level of theory. Spartan '08*, build 132 (Mar 27 2009), Wavefunction Inc., Irvine CA, 2009; (b) T. A. Halgren, *J. Comput. Chem.*, 1996, **17**, 490–519.
- 22 (a) A. Mirabaud, A. Martinez, F. Bayard, J.-P. Dutasta and V. Dufaud, *New J. Chem.*, 2018, **42**, 16863–16874; (b) J. Wang, Y. Liang, D. Zhou, J. Ma and H. Jing, *Org. Chem. Front.*, 2018, **5**, 741–748; (c) A. Mirabaud, J.-C. Mulatier, A. Martinez, J.-P. Dutasta and V. Dufaud, *Catal. Today*, 2017, **281**, 387–391; (d) A. Mirabaud, J.-C. Mulatier, A. Martinez, J. P. Dutasta and V. Dufaud, *ACS Catal.*, 2015, **5**, 6748–6752.
- 23 (a) C. Maeda, S. Sasaki, K. Takaishia and T. Ema, *Catal. Sci. Technol.*, 2018, **8**, 4193–4198; (b) L. Martínez-Rodríguez, J. O. Garmilla and A. W. Kleij, *ChemSusChem*, 2016, **9**, 749–755; (c) J. Shi, J. Song, J. Ma, Z. Zhang, H. Fan and B. Han, *Pure Appl. Chem.*, 2013, **85**, 1633–1641; (d) J. Song, Z. Zhang, B. Han, S. Hu, W. Li and Y. Xie, *Green Chem.*, 2008, **10**, 1337–1341.
- 24 W. Desens, C. Kohrt, M. Frank and T. Werner, *ChemSusChem*, 2015, **8**, 3815–3822.
- 25 L. Wang, G. Zhang, K. Kodama and T. Hirose, *Green Chem.*, 2016, **18**, 1229–1233.
- 26 (a) C. Chen, J. Zhang, G. Li, P. Shen, H. Jin and N. Zhang, *Dalton Trans.*, 2014, **43**, 13965–13971; (b) Z. Z. Yang, L. N. He, Y. N. Zhao, B. Li and B. Yu, *Energy Environ. Sci.*, 2011, **4**, 3971–3975; (c) J. C. Meredith, K. P. Johnston, J. M. Seminario, S. G. Kazarian and C. A. Eckert, *J. Phys. Chem.*, 1996, **100**, 10837–10848.
- 27 (a) K. A. Andrea and F. M. Kerton, *ACS Catal.*, 2019, **9**, 1799–1809; (b) P. Yingcharoen, C. Kongtes, S. Arayachukiat, K. Suvarnapunya, S. V. C. Vummaleti, S. Wannakao, L. Cavallo, A. Poater and V. D'Elia, *Adv. Synth. Catal.*, 2019, **361**, 366–373; (c) O. Sodpiban, S. Del Gobbo, S. Barman, V. Aomchad, P. Kidkhunthod, S. Ould-Chikh, A. Poater, V. D'Elia and J.-M. Basset, *Catal. Sci. Technol.*, 2019, **9**, 6152–6165; (d) K. Takaishi, T. Okuyama, S. Kadosaki, M. Uchiyama and T. Ema, *Org. Lett.*, 2019, **21**, 1397–1401; (e) X. Wu, C. Chen, Z. Guo, M. North and A. C. Whitwood, *ACS Catal.*, 2019, **9**, 1895–1906; (f) S. Arayachukiat, C. Kongtes, A. Barthel, S. V. C. Vummaleti, A. Poater, S. Wannakao, L. Cavallo and V. D'Elia, *ACS Sustainable Chem. Eng.*, 2017, **5**, 6392–6397.
- 28 S. Liu, N. Suematsu, K. Maruoka and S. Shirakawa, *Green Chem.*, 2016, **18**, 4611–4615.
- 29 N. Liu, Y.-F. Xie, C. Wang, S.-J. Li, D. Wei, M. Li and B. Dai, *ACS Catal.*, 2018, **8**, 9945–9957.
- 30 (a) W. Clegg, R. W. Harrington, M. North and R. Pasquale, *Chem. – Eur. J.*, 2010, **16**, 6828–6843; (b) M. North and R. Pasquale, *Angew. Chem., Int. Ed.*, 2009, **48**, 2946–2948.
- 31 (a) L. Wang, C. Xu, Q. Han, X. Tang, P. Zhou, R. Zhang, G. Gao, B. Xu, W. Qin and W. Liu, *Chem. Commun.*, 2018, **54**, 2212–2215; (b) C. J. Whiteoak, N. Kielland, V. Laserna, E. C. Escudero-Adán, E. Martin and A. W. Kleij, *J. Am. Chem. Soc.*, 2013, **135**, 1228–1231.
- 32 (a) I. Martí, M. Bolte, M. I. Burguete, C. Vicent, I. Alfonso and S. V. Luis, *Chem. – Eur. J.*, 2014, **20**, 7458–7464; (b) I. Martí, J. Rubio, M. Bolte, M. I. Burguete, C. Vicent, R. Quesada, I. Alfonso and S. V. Luis, *Chem. – Eur. J.*, 2012, **18**, 16728–16741.
- 33 (a) G. Pescitelli, L. Di Bari and N. Berova, *Chem. Soc. Rev.*, 2011, **40**, 4603–4625; (b) B. Ranjbar and P. Gill, *Chem. Biol. Drug Des.*, 2009, **74**, 101–120; (c) B. M. Bullheller, A. Rodger and J. D. Hirst, *Phys. Chem. Chem. Phys.*, 2007, **9**, 2020–2035; (d) S. M. Kelly, T. J. Jess and N. C. Price, *Biochim. Biophys. Acta*, 2005, **1751**, 119–139; (e) S. M. Kelly and N. C. Price, *Curr. Protein Pept. Sci.*, 2000, **1**, 349–384.
- 34 (a) H. Guo, L.-W. Zhang, H. Zhou, W. Meng, Y.-F. Ao, D.-X. Wang and Q.-Q. Wang, *Angew. Chem., Int. Ed.*, 2020, **59**, 2623–2627; (b) N. H. Evans and P. D. Beer, *Angew. Chem., Int. Ed.*, 2014, **53**, 11716–11754; (c) D. K. Cabbiness and D. W. Margerum, *J. Am. Chem. Soc.*, 1969, **91**, 6540–6541.
- 35 I. Alfonso, M. I. Burguete, F. Galindo, S. V. Luis and L. Vígara, *J. Org. Chem.*, 2007, **72**, 7947–7956.
- 36 N. A. Tappe, R. M. Reich, V. D'Elia and F. E. Kühn, *Dalton Trans.*, 2018, **47**, 13281–13313.